

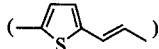
Calculations on the Nonlinear Second-Order Optical Polarizabilities for Series of Donor-C₆₀ Molecules

LIU, Xiao-Juan^a(刘孝娟) FENG, Ji-Kang^{*,a,b}(封继康) REN, Ai-Min^a(任爱民)
 ZHOU, Xin^a(周新)

^a State Key Laboratory of Theoretical and Computational Chemistry, Institute of Theoretical Chemistry, Jilin University, Changchun, Jilin 130023, China

^b The College of Chemistry, Jilin University, Changchun, Jilin 130023, China

The equilibrium geometries and UV-visible spectra of a series of donor-C₆₀ molecules were obtained by means of the AM1 and INDO/CI method, on the basis of accurate geometric and electronic structures. The nonlinear second-order optical polarizabilities were calculated using the method INDO/SDCI combined with the Sum-Over-States (SOS) expression. The calculated β ($\lambda = 1.34 \mu\text{m}$) values are 28.81, 48.56, 57.33, 66.99, 70.85, 85.84, and 142.14 ($\times 10^{-30}$ esu) for the molecules A, B, C, D, E, F and G, respectively. The frontier orbitals were plot for the representative molecules in order to exhibit the intramolecular charge transfer. The results indicate that introduction of thienylethylene



can enhance the NLO response and the dimethylaniline-substituted dithienylethylene-C₆₀ (molecule G) possesses the largest NLO second-order optical polarizability. The large β values can be attributed to the charge transfer between the substituents and C₆₀, as well as within the three-dimensional conjugated sphere of C₆₀.

Keywords INDO/SDCI, nonlinear second-order polarizability, SOS expression

Introduction

The bulk preparation¹ of C₆₀ and C₇₀ clusters (fullerenes) has stimulated a wide variety of experimental and theoretical studies.²⁻⁵ We have successfully examined the structures, UV-visible spectra and the nonlinear third-order optical polarizabilities (γ) of C₆₀ and C₇₀.^{6,7} By introduction of substituents, the centrosymmetries of C₆₀ and C₇₀ are broken and the second-order optical nonlinearities are induced. The charge separation in substituted C₆₀ which leads to enhancement of β value has also been discussed.⁵

In recent years, a number of electron donors such as porphyrin, ferrocene, and *N,N*-dimethylaminophenyl have been covalently linked to the C₆₀ cage by different synthetic procedures⁸ in an effort to obtain efficient intramolecular electron or charge transfer and to generate

long-lived charge-separated states in these donor-acceptor (D-A) molecular assemblies.⁹⁻¹⁷ Furthermore, nanocomposite materials containing fullerenes for optical application have been synthesized to achieve the best control of fullerene interactions in different environments and higher fullerene dispersions in solid environments.¹⁸ Diekers *et al.*^{19a} recently pointed out that three types of dyads and triads involving a C₆₀ moiety with various donor molecules have been developed. Francis *et al.*^{19b} reported that fullerene bearing redox active groups which undergo reversible redox reactions may be more suitable for building molecular charge storage devices than pristine fullerenes. Although spontaneous intramolecular charge-transfer (ICT) interactions have been claimed in some cases, cogent evidences are still lacking, such as the relationship between the ICT properties and the molecular structures. Based on this idea, in an attempt to enhance intramolecular electron or charge transfer, Liu *et al.*²⁰ synthesized a novel donor-C₆₀ involving dimethylaniline-substituted dithienylethylene (DADTE) as the donor part and investigated its optical and electrochemical properties experimentally. But, few theoretical studies on the nonlinear second-order polarizabilities of these compounds have been reported. In this paper, we designed seven molecules (A, B, C, D, E, F and G, see Fig. 1) based on acceptor-donor structures with C₆₀ as the acceptor, and thiophene, one or two thienylethylene and/or dimethylaniline as donors. Their equilibrium geometries were obtained with AM1 method, and the UV-visible spectra were calculated by the INDO/SDCI, on the basis of the optimized geometries and UV-visible spectra. The nonlinear second-order (NLO) optical polarizabilities of all the designed molecules were calculated by INDO/SDCI-SOS method. The calculated values of β_{μ} are 28.81, 48.56, 57.33, 66.99, 70.85, 85.84, and 142.14 ($\times 10^{-30}$ esu) for the molecules A, B, C,

* E-mail: Jikangf@yahoo.com

Received November 26, 2002; revised and accepted February 24, 2003.

Project supported by the National Science Foundation of China (Nos. 20273023, 90101026) and the Key Laboratory for Supramolecular Structure and Material of Jilin University.

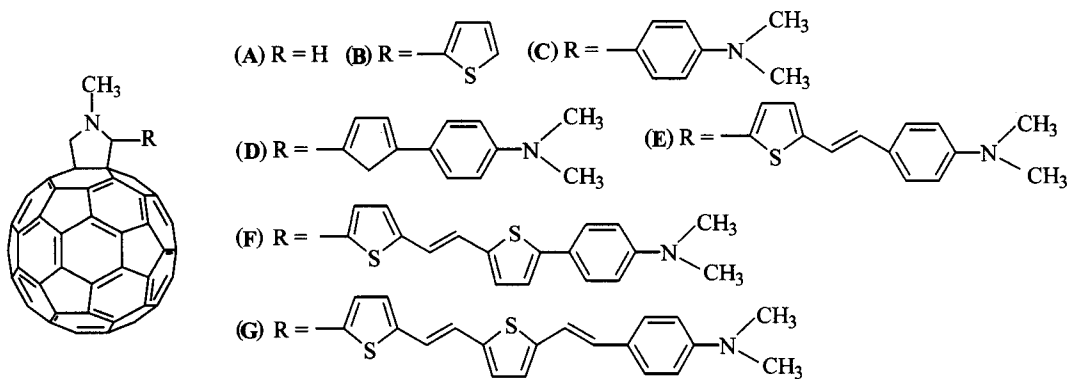


Fig. 1 The series of investigated donor-C₆₀ molecules.

D, E, F and G, respectively, indicating that introduction of thienylethylene could enhance the NLO response. All the calculations were intended to give a clear insight into the molecular NLO response of the investigated molecules.

Theoretical method

The quantitative description of molecular NLO response is derived from a power series expansion of the molecular polarization upon interaction with an external oscillating electromagnetic field

$$P_i = \sum_j \alpha_{ij} E_j + \sum_{jk} \beta_{ijk} E_j E_k + \sum_{jkl} \gamma_{ijkl} E_j E_k E_l + \dots (1)$$

$$\beta_{ijk} + \beta_{ikj} = \frac{1}{4\hbar^2} \left\{ \sum_{\substack{n \neq n' \\ n' \neq g}} \left[\begin{aligned} & (r_{gn'}^j r_{n'n}^i r_{gn}^k + r_{gn'}^k r_{n'n}^i r_{gn}^j) \times \left(\frac{1}{(\omega_{n'g} - \omega)(\omega_{ng} + \omega)} + \frac{1}{(\omega_{n'g} + \omega)(\omega_{ng} - \omega)} \right) \right. \\ & + (r_{gn'}^j r_{n'n}^j r_{gn}^k + r_{gn'}^k r_{n'n}^j r_{gn}^j) \times \left(\frac{1}{(\omega_{n'g} - 2\omega)(\omega_{ng} - \omega)} + \frac{1}{(\omega_{n'g} + 2\omega)(\omega_{ng} + \omega)} \right) \\ & \left. + (r_{gn'}^j r_{n'n}^k r_{gn}^i + r_{gn'}^k r_{n'n}^i r_{gn}^j) \times \left(\frac{1}{(\omega_{n'g} - \omega)(\omega_{ng} - 2\omega)} + \frac{1}{(\omega_{n'g} + \omega)(\omega_{ng} + 2\omega)} \right) \right] \right. \\ & \left. + 4 \sum_{n \neq g} [r_{gn'}^j r_{n'n}^k \Delta_m^i (\omega_{ng}^2 - 4\omega^2) + r_{gn}^j (r_{gn'}^k \Delta_n^i + r_{gn}^j \Delta_n^k) (\omega_{ng}^2 + 2\omega^2)] \left(\frac{1}{(\omega_{ng}^2 - \omega^2)(\omega_{ng}^2 - 4\omega^2)} \right) \right\} (2)$$

where the summations are over the complete sets of eigenstates $|n\rangle$ and $|n'\rangle$ of the unperturbed molecular system. The quantities r_{gn}^i and $r_{n'n}^i$ are matrix elements of the i th components of the dipole operator between the unperturbed ground and excited states and between the two excited states, respectively; $\Delta_n^i = r_{nn}^i - r_{gg}^i$ is the difference between the excited-state and ground-state dipole moments; ω , the frequency of the applied electric field; $\hbar\omega_{ng}$, the difference between the excited-state and the ground-state energies. Although all 27 components of the β tensor can be computed, only the vector component in the dipolar direction (β_μ) is sampled by electric field-induced second harmonic generation (EFISH) experiments. β_μ is given by

$$\beta_\mu(-2\omega; \omega, \omega) = \sum_{i=1}^3 (\mu_i \beta_i / |\mu|) (3)$$

where

$$\beta_i = \beta_{iii} + \frac{1}{3} \sum_{j \neq i} (\beta_{ijj} + \beta_{jij} + \beta_{jji}) \quad i, j \in (x, y, z) (4)$$

The all-valence INDO/CI (intermediate neglect of differential overlap) technique was employed to provide the transition dipole moment and the transition energy needed in the SOS expression (2). In the computation, 17 highest occupied and 17 lowest unoccupied orbitals were included in the single (S) excitation, in addition to

Here, P_i is the molecular polarization induced along the i th axis, E_j is the j th component of the applied electric field, α is the linear polarizability, β is the first hyperpolarizability or the second-order polarizability, and γ is the second hyperpolarizability or the third-order polarizability. α , β and γ describe the responsivity of the molecule to an electromagnetic perturbation and are constants for a given molecular geometry and external electromagnetic field. The β and γ are responsible for second-harmonic and third-harmonic generation. The Sum-Over-States (SOS) expression for the individual components of the second-order polarizability tensor has been given from perturbation theory²¹ as Eq. (2)

two highest occupied and two lowest unoccupied orbitals in the double (D) excitation. All together there were 335 excitations in the CI calculations.

Results and discussion

Design of the molecules and the geometry optimization

Based on molecule **A** (C_{60} /pyrrolidine), by substitution with thienylene, dimethylaniline and thienyldimethylaniline, molecules **B**, **C** and **D** are formed, respectively; on the basis of molecule **C**, the introduction of one or two thienylethylene results in molecules **E** or **G**; similarly one thienylethylene were inserted in **D** to form molecule **F**.

By using the AM1 method, the geometries of molecules **A**–**G** were optimized. The equilibrium geometry of C_{60} have been also obtained at the same level, and the results are: $R_{6-6} = 0.1385$ nm and $R_{5-6} = 0.1460$ nm, which were in good agreement with NMR experiment.²² Taking molecule **G** as an example, their optimized bond length parameters are shown in Fig. 2(a). The pyrrolidine ring is fused with C_{60} with a 6,6-ring conjugation. With the introduction of the additional groups, the C(18)–C(28) bond becomes a single bond with bond length (BL) of 0.1576 nm, compared with the 6,6-bond length of 0.1385 nm. Thus C(18)–C(28) protrudes from C_{60} sphere, which causes the entire surrounding C–C bonds to be stretched. As shown in Fig. 2(a), the bond lengths are 0.1525, 0.1527, 0.1525 and 0.1525 nm for the bonds C(28)–C(38), C(28)–C(31), C(18)–C(17) and C(18)–C(10), respectively. In the pyrrolidine part, the bond length of C(18)–C(61) is 0.1576 nm and that of C(28)–C(62) is 0.1554 nm. For the other bonds in the C_{60} part, the further the bond is from the bond C(18)–C(28), the less the bond length is changed, compared with the corresponding one in C_{60} . As shown in Fig. 2, the BL of C(49)–C(50) is 0.1385 nm which is almost unchanged. The AM1 calculation shows that the distance between C(18) and the center of the C_{60} sphere is 0.4090 nm, which is longer than 0.3525 nm in the original C_{60} , calculated at the same level.

The lateral figures and the label of molecule **G** are shown in Fig. 2(b) which indicate that the DADTE part is coplanar. Furthermore, all the double-bond linkages are all-*trans* by the calculation results.

UV-vis spectra

The calculated wavelengths and oscillator strengths of the UV-visible absorptions for molecules **A**–**G** are listed in Table 1, as well as the experimental values of C_{60} for comparison. In Table 1, only those data whose oscillator strength is no less than 0.2 are listed for brief. Taking molecule **G** as an example, we plot the whole UV-visible spectrum, as shown in Fig. 3. The three characteristic

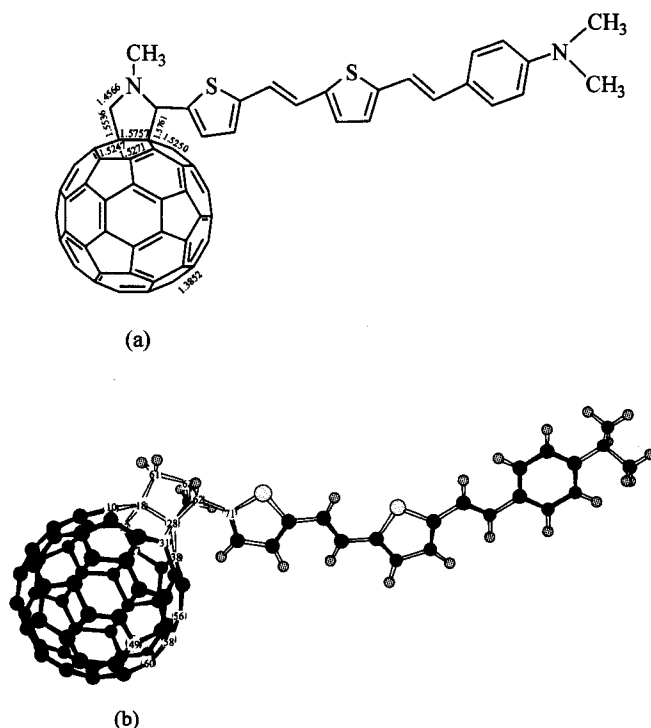


Fig. 2 (a) Optimized geometry parameters of compound **G** and (b) optimized lateral view and the label of compound **G**.

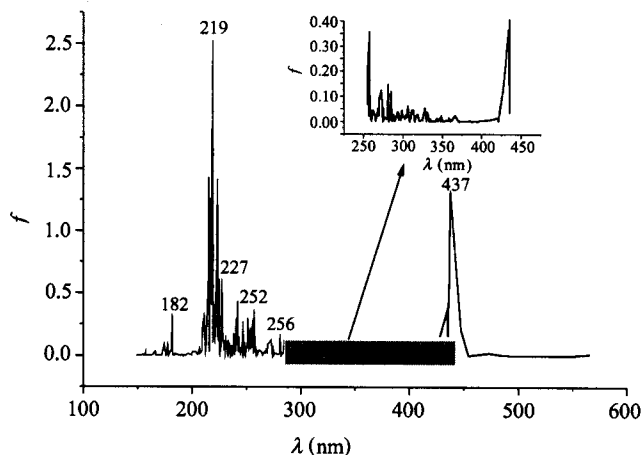


Fig. 3 The UV-visible spectrum of molecule **G** (the inset is the enlarged section of the absorption between 256 nm and 437 nm).

absorption bands of C_{60} in the 200–350 nm region essentially dominate the spectrum of the molecules **A**–**D**. For molecules **E**–**G**, the three strong absorptions are located at 210–219 nm, 223–241 nm and 252–257 nm regions, corresponding to the previous calculated 209, 231 and 245 nm for C_{60} ,⁶ and in good agreement with the experimental 211, 227, and 256 nm, respectively.²³ From molecules **A** to **D**, the absorptions in 210–219 nm and 252–257 nm ranges are red-shifted due to the substituent structures changing from pyrrolidine, thiophene, dimethyl-

Table 1 Calculated wavelengths and oscillator strengths for molecules A—G and experimental values for C₆₀

Compd	Wavelength (nm) and oscillator strength																
A	λ (nm)	257	241	230	226	223	221	220	217	214	211	208					
	f	0.45	0.71	0.85	0.89	2.47	0.83	2.20	0.88	1.17	1.77	2.41					
B	λ (nm)	252	241	240	230	223	223	222	222	221	217	214	211	209			
	f	0.45	0.63	0.52	0.88	0.82	0.68	1.33	0.88	1.78	0.50	0.74	1.48	1.58			
C	λ (nm)	284	257	242	229	225	222	221	221	218	215	213	212	211	208		
	f	0.25	0.33	0.29	0.35	1.27	0.66	2.41	1.63	0.78	0.58	0.69	0.72	1.29	0.55		
D	λ (nm)	338	257	251	243	229	227	224	221	221	220	219	219	212	212	211	210
	f	0.26	0.20	0.32	0.49	0.40	0.41	1.26	1.86	1.42	0.94	0.72	0.52	1.07	1.44	0.50	1.18
E	λ (nm)	374	258	231	228	224	222	221	220	218	216	215	215	214	212	212	
	f	0.51	0.22	0.30	0.70	1.18	0.51	0.81	0.58	2.23	2.12	0.90	0.75	0.74	0.47	0.44	
F	λ (nm)	431	424	257	256	252	242	225	222	220	220	218.4	218.2	217.7	217.0	216.9	216
	f	0.55	0.67	0.23	0.26	0.30	0.33	1.32	0.81	0.57	1.08	1.50	0.78	1.41	0.59	1.65	2.52
G	λ (nm)	437(436) ^a	257	256	251	247	227	225	223	222	220	220	219	218	218	217	215
	f	1.31	0.36	0.27	0.28	0.26	0.60	0.62	1.41	0.45	0.42	0.43	2.54	0.90	1.82	1.26	1.43
C ₆₀	λ^b (nm)	256	227	211													
	λ^c (nm)	245	231	209													

^a 436 is the experimental value; ^b Lit. 23; ^c Lit. 6.

aniline to thienyl-dimethylaniline. Upon introduction of the larger moiety in the structure, a broad and intense absorption band developed in the region of 370–440 nm for molecules E–G, which does not exist for pristine C₆₀. For molecules E–G, the λ_{\max} was red-shifted. For example, λ_{\max} of molecule G (substituted by DADTE) was 437 nm, which is in good agreement with the experimental value of 436 nm. In later analysis, we found that this absorption was connected with the charge transfer between C₆₀, dimethylaniline and the dithienylethylene.

NLO properties

On the basis of the optimized geometries and electronic spectra, the nonlinear second-order optical polarizabilities β_{ijk} and β_{μ} were calculated by use of the INDO/SDCI-SOS method.

In the SOS expression [Eq. (2)] for β , the summation is over the complete sets of eigenstates $|g\rangle$, $|n\rangle$, and $|n'\rangle$ of the unperturbed system. They have to be truncated in practical calculations for feasibility. In Eq. (2), the denominator of each term includes ω_{ng} , $\omega_{n'g}$. When n and n' increase, the energy differences between the ground state and the excited states will increase, *i. e.*, the denominator will increase more and more. It means that the contribution to β will become less important when n and n' reach a certain value. Li *et al.*⁶ demonstrated that 197 excited states were found to be sufficient for effective convergence for C₆₀. We considered that the investigated molecules were more complicated than C₆₀, so it is necessary to include 335 configurations (SDCI) in the calculations of β . Fig. 4 illustrates the relationship between the number of the excited states involved and the values of β_{μ} ($\lambda = 1.34 \mu\text{m}$), which indicates that β_{μ} values converge when the numbers of excited states reach

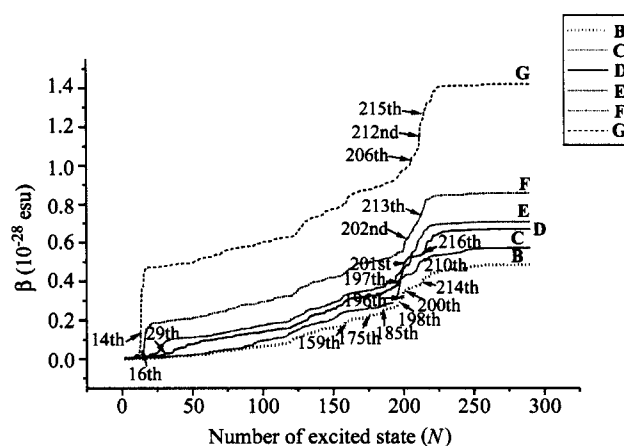


Fig. 4 Plots of β value versus the number of excited states for molecules B–G.

250. The converged absolute value of λ_{μ} is simplified as β . The value of β is related to β , the laser field frequency, (here λ was taken at $1.34 \mu\text{m}$) and the calculated second-order optical polarizabilities are expected to be mostly free of resonance enhancement (see the discussion about dispersion in the latter section). The converged values of β are listed in Table 2,²⁵ as well as values of β_0 obtained by taking λ to be zero in the calculation. C₆₀/Diethylamino, which had been measured in experiment,²⁴ was chosen for comparison. According to the substituent strength in organic chemistry, diethylamino is almost the same with dimethylamino as the substituent of molecule C. Furthermore, for all the molecules the β value showed: $\beta_7 > \beta_6 > \beta_5 > \beta_4 > \beta_3 > \beta_2 > \beta_1$. As we expected, the introduction of thiophene (B) and dimethylaniline (C) leads to larger second-order NLO responses, which is due to the greater electron delocalization and donating effect, respectively. For molecule D, the combined effects of electron

Table 2 Calculated results of β (10^{-30} esu) for the investigated compounds

Compd	A	B	C	D	E	F	G	C_{60}/DEA_{exp}^a
β ($\lambda = 1.34 \mu\text{m}$)	28.81	48.56	57.33	66.99	70.85	85.84	142.14	67 ± 20 ($\lambda = 1.91 \mu\text{m}$)
β_0 ($\lambda = 0$)	27.27	45.87	54.15	62.90	66.22	78.93	128.70	

^a see Lit. 24.

delocalization and donating results in larger NLO responsibility than those of molecules **B** and **C**. From molecule **C** to **E** and **G**, the molecules were inserted one thienylenthylene in succession, which is equal to increasing conjugation bridge length and enlarging the conjugation extent, and the values of β are 57.33, 70.85, 142.14 ($\times 10^{-30}$ esu), respectively, indicating that the group of thienylenthylene is a good conjugated bridge for NLO materials. For molecules **D** and **F**, the same results can also be obtained. Furthermore, the introduction of thiophene generally will make the molecules possess high thermal and photochemical stabilities.²⁵ We will further discuss the original reason micromechanically in the following.

Fig. 4 illustrates that β accumulates up to 250 excited states for all the investigated molecules. For molecules **B–D**, only the high-energy excited states make contributions to β , while for molecules **E–G**, not only the high-energy excited states but also the low-energy excited states make contribution to β .

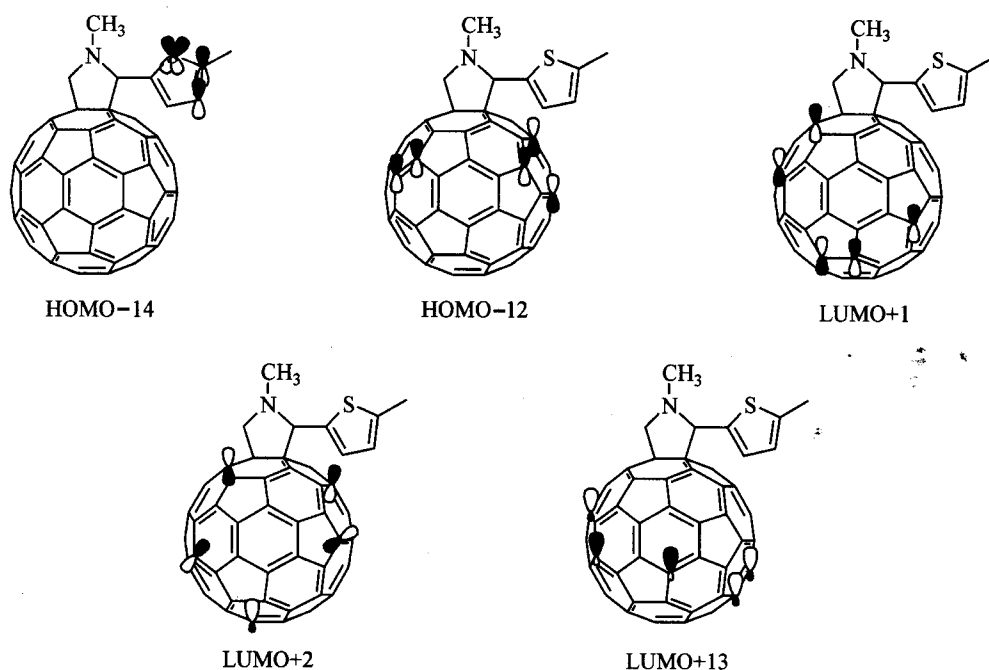
In 1957, Oudar^{26,27} developed the famous two-level approximation as bellow

$$\beta_{\mu} = \frac{3e^2\hbar^2}{2m} \frac{Wf\Delta\mu}{[W^2 - (2\hbar\omega)^2][W^2 - (\hbar\omega)^2]} \quad (5)$$

where ω is the frequency of the laser field, $W = \hbar\omega_n$ is the transition energy from ground state to a specific excited

state n , f is the oscillator strength of the transition, and $\Delta\mu$ is the difference of dipole moments between the excited and ground states. Eq. (5) clearly indicates the contribution of an excited state to β . We took molecules **B** and **G** as examples to illustrate the essential reasons for the NLO response micromechanically.

For molecule **B** with thiophene as substituent, the 159th, 175th, 185th, 198th, 200th and 214th excited states evidently contribute to β as shown in Fig. 4. According to the two-state approximation formula (5), the contribution of these excited states to β are 3×10^{-30} , 1×10^{-30} , 1×10^{-30} , 2×10^{-30} , 3×10^{-30} and 3×10^{-30} esu respectively. The 198th excited state is mainly a mixture of HOMO - 14 \rightarrow LUMO + 2 and HOMO - 12 \rightarrow LUMO + 13; similarly the 200th excited state is mainly made up of HOMO - 14 \rightarrow LUMO + 1. In Fig. 5, we plot the orbitals of HOMO - 14, HOMO - 12, LUMO + 1, LUMO + 2 and LUMO + 13 to visually show charge transfer in molecule **B**. It is obvious that the transition from HOMO - 14 \rightarrow LUMO + 2 and HOMO - 14 \rightarrow LUMO + 1 are equal to the charge transfer from the substituent to C_{60} , while the transition from HOMO - 12 \rightarrow LUMO + 13 can be considered as the charge transfer within the C_{60} sphere. The result indicates that the C_{60} part acts as the acceptor, furthermore, the charge transfer from the substituent to C_{60} makes a large contribution to the NLO response in molecule **B**.

**Fig. 5** Frontier orbitals of molecule **B**.

For molecule **G** with DADTE as the substituent, Fig. 4 showed that the 14th, 206th, 211th, 212th, 215th and 220th excited states make considerable contributions to β , and according to the two-state formula, their contributions to β are 7×10^{-30} , 2×10^{-30} , 8×10^{-30} , 5×10^{-30} , 3×10^{-30} and 4×10^{-30} esu respectively. The 14th excited state, in the low-lying energy, is mostly made up of HOMO - 1 \rightarrow LUMO + 2 and HOMO \rightarrow LUMO + 3; and the 212th excited state, one of the high-lying energy excited states, is mainly a mixture of HOMO - 11 \rightarrow LUMO + 12 and HOMO - 9 \rightarrow LUMO + 16. The 14th excited state is equal to the charge transfer between C₆₀ and the substituent, while the transition of HOMO - 11 \rightarrow LUMO + 12 and HOMO - 9 \rightarrow LUMO + 16 of the 212th excited state can be viewed as the charge transfer within the C₆₀ sphere. In order to further specify the mechanism of the NLO responsibility of molecule **G**, we also calculated the net charge quantities of the ground and the 14th excited state as shown in Fig. 6. Fig. 6 shows that for both ground and excited states, C₆₀ possesses negative charge, indicating that C₆₀ is the acceptor in the donor-C₆₀ compound. The charge transfer between the donor and acceptor, which is responsible for the NLO response, is due to the conjugative effect between them.

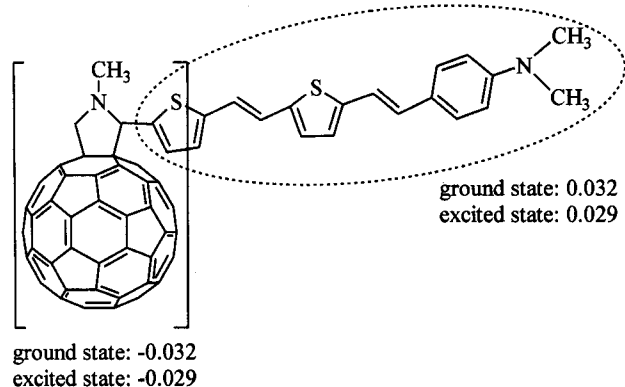


Fig. 6 Net charge of the ground and the main excited state for molecule **G**.

Taking molecule **G** as an example, we investigated the dispersion of β (shown in Fig. 7). Fig. 7 displays the relationship between the value of β and the applied field

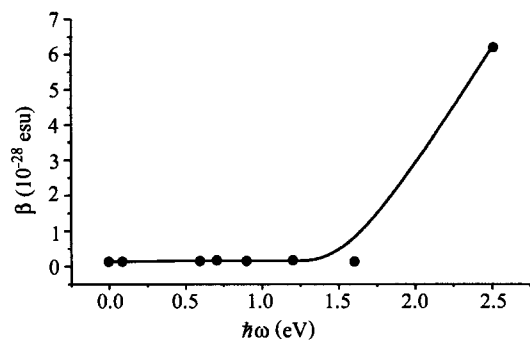
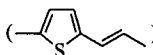


Fig. 7 Calculated dispersion of β_{μ} for compound **G**.

in eV. The calculated data can be extrapolated to zero static quantity β (0;0,0). We take $\lambda = 1.34 \mu\text{m}$ (0.93 eV) in all calculations, and it is in the nonresonant area.

Conclusion

With the INDO/SDCI-SOS method, we calculated the optical second-order nonlinearities of a series of donor-acceptor compounds based on C₆₀. The results show that the introduction of the thienylethylene () can

enhance the NLO response. Furthermore, with the substituent becoming larger, that is increasing the conjugation length, both the low-lying excited states and the high-lying ones make contributions to the NLO response. In these compounds, C₆₀ acts as the acceptor and charge transfers occur during the NLO response.

References

- Krätschmer, W.; Lamb, L. D.; Fostiropoulos, K.; Guffman, D. R. *Nature* **1990**, *347*, 354.
- Wang, Y.; Cheng, L. J. *Phys. Chem.* **1992**, *96*, 1530.
- Wang, Y. *J. Phys. Chem.* **1992**, *96*, 764.
- Palit, D. K.; Ghosh, H. N.; Pal, H.; Sapre, A. V.; Mittal, J. P.; Seshadri, R.; Rao, C. N. R. *Chem. Phys. Lett.* **1992**, *198*, 113.
- Matsuzawa, N.; Dixon, D. A.; Fukunaga, T. *J. Phys. Chem.* **1992**, *96*, 7594.
- Li, J.; Feng, J.; Sun, J. *J. Chem. Phys. Lett.* **1993**, *203*, 560.
- Li, J.; Feng, J. K.; Sun, C. C. *Int. J. Quantum Chem.* **1994**, *52*, 673.
- Recent reviews related to C₆₀-based donor-acceptor molecular assemblies:
 - Martin, N.; Sánchez, L.; Illescas, B.; Pérez, I. *Chem. Rev.* **1998**, *98*, 2527.
 - Prato, M.; Maggini, M. *Acc. Chem. Res.* **1998**, *31*, 519.
 - Prato, M. *J. Mater. Chem.* **1997**, *7*, 1097.
 - Diederich, F.; Gómez-López, M. *Chem. Soc. Rev.* **1999**, *28*, 263.
- (a) Guldi, D. M. *Chem. Commun.* **2000**, 321.
(b) Guldi, D. M.; Prato, M. *Acc. Chem. Res.* **2000**, *33*, 695.
(c) Drovetskaya, T.; Reed, C. A.; Boyd, P. *Tetrahedron Lett.* **1995**, *36*, 7971.
(d) Linssen, T. G.; Dürr, K.; Ganack, M.; Girsch, A. *J. Chem. Soc., Chem. Commun.* **1995**, 103.
(e) Qiu, W. F.; Liu, Y. Q.; Zhu, D. B. *Chin. Chem. Lett.* **1997**, *8*, 363.
- Maggini, M.; Karlssin, A.; Scorrano, G.; Sandomà, G.; Farnia, G.; Prato, M. *J. Chem. Soc., Chem. Commun.* **1994**, 589.
- Martín, N.; Sánchez, L.; Seoane, C.; Andreu, R.; Garín,

- J. Orduña, J. *Tetrahedron Lett.* **1996**, *37*, 5979.
- 12 (a) Llacay, J.; Mas, M.; Molins, E.; Veciana, J.; Powell, D.; Rovira, C. *J. Chem. Soc., Chem. Commun.* **1997**, 659.
(b) Llacay, J.; Veciana, J.; Vidal-Gancedo, J.; Bourdelande, J. L.; Gonzalez-Moreno, R.; Rovira, C. *J. Org. Chem.* **1998**, *63*, 5220.
(c) Bouille, C.; Rabreau, J. M.; Hudhomme, P.; Cariou, M.; Jubault, M.; Gorgues, A.; Orduna, J.; Garin, J. *Tetrahedron Lett.* **1997**, *38*, 3909.
- 13 Lawson, J. M.; Oliver, A. M.; Rothenfluh, D. F.; An, Y. Z.; Ellis, G. A.; Ranasinghe, M. G.; Khan, S. I.; Franz, A. G.; Ganaphthi, P. S.; Stephard, M. J.; Paddonrow, M. N.; Rubin, Y. *J. Org. Chem.* **1996**, *61*, 5032.
- 14 Matsubara, Y.; Tada, H.; Nagase, S.; Yoshida, Z. *J. Org. Chem.* **1995**, *60*, 5372.
- 15 Nakamura, Y.; Minowa, T.; Tobita, S.; Shizuka, H.; Nishimura, J. *J. Chem. Soc., Perkin Trans.* **1995**, *2*, 2351.
- 16 Williams, R. M.; Koeberg, M.; Lawson, J. M.; An, Y. Z.; Rubin, Y.; Paddon-Row, M. N.; Verhoeven, J. W. *J. Org. Chem.* **1996**, *61*, 5055.
- 17 Güldi, D. M.; Maggini, M.; Scorrano, G.; Prato, M. *J. Am. Chem. Soc.* **1997**, *119*, 974.
- 18 Brusatin, G.; Signorini, R. *J. Mater. Chem.* **2002**, *12*, 1964.
- 19 (a) Diekers, M.; Girsch, A.; Pyo, S.; Rivera, J.; Echegoyen, L. *Eur. J. Org. Chem.* **1998**, 1111 and references therein.
(b) D'Souza, F.; Zandler, M. E.; Smith, P. M.; Deviprasad, G. R. *J. Phys. Chem. A* **2002**, *106*, 649.
- 20 Liu, S. G.; Shu, L. H.; Rivera, J.; Liu, H. Y.; Raimundo, J. M.; Jean, R.; Alain, G.; Luis, E. *J. Org. Chem.* **1999**, *64*, 4884.
- 21 Teng, C. C.; Garito, A. F. *Phys. Rev. Lett.* **1983**, *50*, 350.
- 22 Yannoni, C. S.; Bernier, P. P.; Bethune, D. S.; Meijer, G.; Salem, J. R. *J. Am. Chem. Soc.* **1991**, *113*, 354.
- 23 Ajie, H.; Alvarez, M. M.; Anz, S. J.; Beck, R. D.; Diederich, F.; Fostiropoulos, D.; Huffman, D. R.; Krätschmer, W.; Rubin, Y.; Schriver, D. E.; Sensharma, D.; Whetten, R. L. *J. Phys. Chem.* **1990**, *94*, 8630.
- 24 Wang, Y.; Cheng, L. *J. Phys. Chem.* **1992**, *96*, 1530.
- 25 Irie, M.; Miyatake, O.; Uchida, K.; Eriguchi, T. *J. Am. Chem. Soc.* **1994**, *116*, 9894.
- 26 Oudar, J. L.; Chemla, D. S. *J. Chem. Phys.* **1977**, *66*, 2664.
- 27 Oudar, J. L. *J. Chem. Phys.* **1977**, *67*, 446.

(E0211262 PAN, B. F.; LING, J.)